Robotica (2009) volume 27, pp. 663–676. © 2008 Cambridge University Press
doi:10.1017/S0263574708005031 Printed in the United Kingdom

A novel spherical parallel manipulator: forward position problem, singularity analysis, and isotropy design

Javad Enferadi†* and Alireza Akbarzadeh Tootoonchi‡

†*Department of Mechanical Engineering, Ferdowsi University of Mashhad, Mashhad, Iran.*
‡*Department of Mechanical Engineering, Ferdowsi University of Mashhad, Mashhad, Iran.*

(Received in Final Form: July 22, 2008. First published online: September 8, 2008)

SUMMARY
In this paper, a novel spherical parallel manipulator and its isotropic design is introduced. This manipulator has good accuracy and relatively a larger workspace which is free of singularities. Utilizing spherical configuration the forward position problem is solved by equivalent angle–axis representation and Bezout's method which leads to a polynomial of degree 8. Two examples are given, one for isotropic and one for nonisotrpoic design. The first case results in eight real solutions, therefore, the polynomial being minimal. Using invariant form, we study acceleration analysis, conditions for singularity and find infinite isotropic structures. Accuracy and workspace analysis are also performed and are shown to have good global conditioning index and relatively large workspace. Using isotropic design and singularity requirements, we show the workspace of isotropic design is free of singularity.

KEYWORDS: Spherical parallel manipulator; Forward position problem; Bezout's elimination method; Isotropy design; Singularity analysis.

1. Introduction

Orientating a rigid body without changing its position is required in many technical applications. A spherical manipulator is one in which the end-effector is moved on the surface of a sphere. Therefore, a spherical manipulator can be used as a device to orient the end-effector. Spherical manipulators can be either serial[1] or parallel.[3–13] Serial manipulators feature an open kinematics chain whose ending link is the end-effector. Parallel manipulators are made of two rigid bodies, one moveable (platform) and the other fixed (base), connected to each other by a number of kinematic chains (legs). The moving platform and the fixed base are the end-effector and the base frame, respectively. In each leg, the number of actuated kinematic pairs is less than the total number of kinematic pairs. All legs contribute in carrying the external loads applied to the moving platform. Parallel architectures are usually more stiff and precise than the serial ones, however their structures are more complex.

Alici and Shirinzadeh[7] proposed a spherical parallel manipulator, 3-SPS, which is made of three identical moving legs and a fixed leg. Each of the three moving legs is made of SPS (spherical–prismatic–spherical) joints. The fixed leg joins the moving platform to the base with a passive spherical joint at the moving platform. The prismatic pairs are the actuated joints. Innocenti and Parenti-Castelli,[8] Wohlhart,[9] and Vertechy and Parenti-Castelli[14] have studied a spherical manipulator, 3-UPS, similar to that of Alici and Shirinzadeh.[7] The 3-UPS is also made of three identical moving legs and a fixed leg. Each of the three moving legs is made of UPS (universal–prismatic–spherical) joints. The fixed leg joins the moving platform to the base with a passive spherical joint at the moving platform. The prismatic pairs are the actuated joints. Both manipulators suffer workspace reductions due to the presence of the fixed leg.

Gosselin and others[2–6] have studied a family of overconstrained spherical manipulators with the moving platform and the fixed base connected to one another by either two[6] or three[2–6] legs of type RRR (revolute–revolute–revolute) joints. All legs are located on the surface of an imaginary sphere. Therefore, rotation axes of all revolute pairs converge at a single point which is the center of the sphere. Only one revolute pair per leg is actuated. These manipulators obtain the 3-dof (degrees of freedom) needed for orientating the platform by using repetitive constraints, and the absence of geometric errors is essential to make them work properly.

Karouia and Herve[10] and Di Gregorio[11,12] have studied different types of nonoverconstrained spherical manipulators with three equal legs. This class of spherical manipulators are to be preferred because they do not suffer the overconstrained mechanism troubles and they do not present a passive spherical pair directly joining the platform and the base. These advantages are usually paid for with a more complex structure and the presence of singular configurations (translation singularities) in which the spherical constraint between platform and base fails.

Di Gregorio[13] proposed a new spherical parallel manipulator made of RRS joints. The parallel manipulator is named 3-RRS wrist. The 3-RRS wrist is not overconstrained and exhibits a simple architecture employing three identical legs. Each leg consists of a passive revolute pair, a passive spherical pair, and an actuated revolute pair which is fixed to the base.

Karouia and Hervé[15] proposed an asymmetrical nonoverconstrained 3-dof spherical parallel manipulator.

* Corresponding author. E-mail: Javadenferadi@gmail.com

Each leg is structurally different from other legs. Cervantes-Sanchez *et al.*[16] proposed a symmetrical 2-dof spherical parallel manipulator. It is composed of two legs and five revolute joints.

Mohammadi Daniali *et al.*[17] proposed a double-triangle (DT) spherical parallel manipulator. It consists of two spherical triangles, one fixed and the other moveable. The mechanism consists of three legs. Each leg is made of three joints, PRP (prismatic–revolute–prismatic). Both fixed base and the moving platform are located on the surface of an imaginary sphere. Therefore, axes of all revolute pairs converge at a single point which is the center of the sphere. Only one prismatic joint per leg is actuated.

In this paper, we introduce a novel spherical parallel manipulator that offers some advantages over existing spherical manipulators:

1. Its structural isotropic design exists.
2. It has infinite isotropic structures.
3. Its isotropic design (structure) is free of singularity over the entire workspace.
4. Its isotropic design has a large workspace. The end-effector can travel over the entire fixed base surface.
5. It has good accuracy.

After introducing the novel spherical parallel manipulator, we will solve its forward position problem. Utilizing the spherical configuration of the manipulator and equivalent angle–axis representation two coupled trigonometric equations are obtained. The two coupled equations are solved using Bezout's elimination method which leads to a polynomial of degree 8. Two examples are given, one for the isotropic design and the other for nonisotropic design. The first example utilizes the isotropic design which leads to eight real solutions, the polynomial thus being minimal. The second example is given for the nonisotropic design which leads to four real solutions. Using velocity analysis, we obtain two Jacobian matrices for the manipulator. The two Jacobian matrices are utilized to define three types of singularity conditions and identify the isotropic design. Additionally, it is shown that through changes of only one variable infinite isotropic structures for the novel spherical manipulator may be found. The designer can therefore use this one variable to custom select different size workspace for the task at hand. Finally, we will show all points in the workspace of the isotropic design are free of singularities.

2. Spherical Star-Triangle (ST) Parallel Manipulator

Spherical DT parallel manipulator was introduced by Mohammadi Daniali *et al.*[17] In this paper, we change the moving spherical triangle of the DT to a star, and introduce spherical ST parallel manipulator. This manipulator consists of a fixed spherical triangular base, P, and a moving platform which is shaped like a spherical star, S. The fixed base and the moving platform are connected via three legs. Each of the three moving legs is made of PRP joints. The general model of this manipulator is depicted in Fig. 1. The first prismatic joint which is also the actuated joint moves along a circular arc located on the surface of the sphere. This joint can also be viewed as a revolute joint with its axis passing through the origin of the sphere. Therefore, each of the three moving legs can be thought of being RRP (revolute–revolute–prismatic) joints. In practice, it is difficult to manufacture an actuated prismatic joint which moves on a circular arc. Therefore, to physically construct this manipulator we will build its legs with RRP joints. The physical model of this manipulator is depicted in Fig. 2.

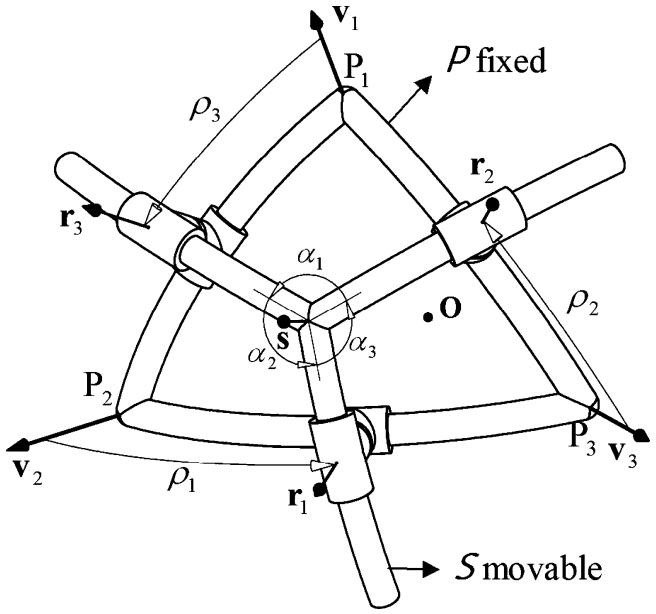

Fig. 1. General model of SST.

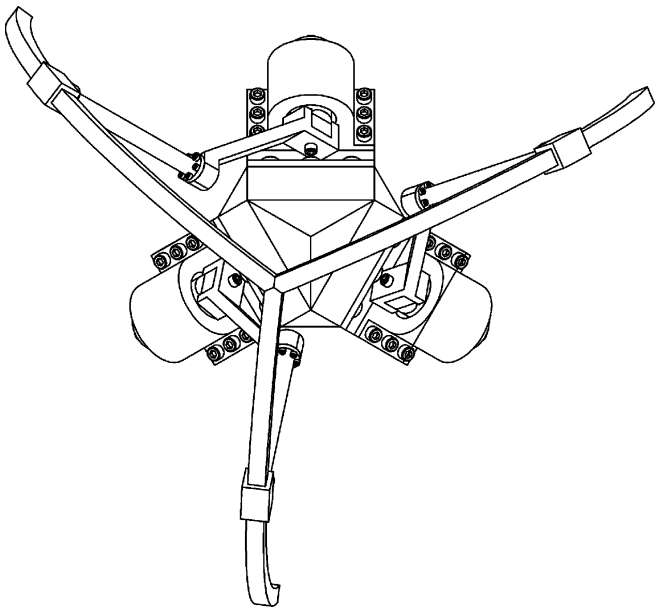

Fig. 2. Spherical star triangle (SST) manipulator.

To develop the mathematical model of the manipulator, first sphere with the center at O and a fixed spherical triangle, $\mathrm{P}_1\mathrm{P}_2\mathrm{P}_3$, on its surface is considered. The P_i corner can be defined by a unit vector, $\mathbf{v}_i$, which starts at P_i and its direction is along OP_i. Actuators stroke which can travel along the arc $\mathrm{P}_{i+1}\mathrm{P}_{i+2}$ is defined by ρ_i. Next, the moveable spherical star, S, is considered. The star is made of three arcs which are located on a surface of a second sphere. The first and the second sphere have the same center but the radius

https://doi.org/10.1017/S0263574708005031 Published online by Cambridge University Press

of the second sphere is slightly larger due to intermediate revolute joint. This difference should be minimized in order to increase the structural stiffness of the manipulator. The three arcs intersect at one point, E, which defines position of the end-effector. This position is mathematically defined by a unit vector, **s**, which starts at the intersections of the three arcs and its direction is along OE. The angle between these arcs, α_1, α_2, and α_3, are manually selected by the robot designer to obtain the desired performance. The arcs of the base triangle, $P_{i+1}P_{i+2}$, cross over the corresponding arcs of the moveable star platform ER_i, at the point R_i. To further define point R_i, unit vector, $\mathbf{r}_i$, which starts at R_i and its direction is along OR_i is defined. Furthermore, R_i is the joint with 2-dof. This joint allows rotation about $\mathbf{r}_i$-axis as well as rotation about the axis that passes through center of sphere, O, and is perpendicular to OER_i plane.

3. Forward Position Problem

In this section, we analyze the forward position problem of spherical ST manipulator. For this purpose, we obtain two trigonometric equations by using the equivalent angle–axis representation and configuration of the manipulator. We previously defined unit vectors that help describe the configuration of robot. Two additional unit vectors, $\mathbf{w}_i$ and $\mathbf{t}_i$ need to be defined in order to describe the position of the passive and actuated prismatic joints. All these unit vectors pass through origin of the sphere. Equivalent angle–axis representation may also be used to define the rotation between these unit vectors. Equivalent angle–axis representation is defined by

$$\mathbf{Q}(\mathbf{e}, \phi) = (\cos\phi)\mathbf{I}_{3\times 3} + (1 - \cos\phi)\mathbf{e}\mathbf{e}^{\mathrm{T}} + (\sin\phi)\mathbf{S}(\mathbf{e}) \tag{1(a)}$$

and

$$\mathbf{S}(\mathbf{e}) = \begin{bmatrix} 0 & -e_z & e_y \\ e_z & 0 & -e_x \\ -e_y & e_x & 0 \end{bmatrix} \tag{1(b)}$$

where ϕ is the angle of rotation, the unit vector **e** is the axis of rotation, e_x, e_y, and e_z are its Cartesian components, and $\mathbf{S}(\mathbf{e})$ is a skew-symmetric matrix. As stated earlier the motion of the prismatic actuator can also be viewed as revolution (revolute joint) with an axis that passes through the origin of the sphere. This axis is defined by a unit vector, $\mathbf{w}_i$. This unit vector is perpendicular to the plane $OP_{i+1}P_{i+2}$ and passes through origin. Therefore,

$$\mathbf{w}_i = \frac{\mathbf{v}_{i+1} \times \mathbf{v}_{i+2}}{\|\mathbf{v}_{i+1} \times \mathbf{v}_{i+2}\|}. \tag{2}$$

The motion of the passive prismatic joint can also be viewed as a revolute joint with an axis that passes through the origin of the sphere. This axis is defined by a unit vector, $\mathbf{t}_i$. This unit vector is perpendicular to the plane OER_i and passes through origin. Therefore,

$$\mathbf{t}_i = \frac{\mathbf{s} \times \mathbf{r}_i}{\|\mathbf{s} \times \mathbf{r}_i\|}. \tag{3}$$

In forward position problem, values of the actuators stroke ρ_i and radius of sphere r are known; therefore, the angle γ_i which is also motor revolution can be defined by

$$\gamma_i = \rho_i / \mathbf{r}, \quad i = 1, 2, 3. \tag{4}$$

If we rotate the unit vector $\mathbf{v}_{i+1}$ about the unit vector $\mathbf{w}_i$ in positive direction by angle γ_i, the unit vector $\mathbf{r}_i$ can be obtained by

$$\mathbf{r}_i = \mathbf{Q}(\mathbf{w}_i, \gamma_i)\mathbf{v}_{i+1} = (\cos\gamma_i)\mathbf{v}_{i+1} + (1 - \cos\gamma_i)\mathbf{w}_i\mathbf{w}_i^{\mathrm{T}}\mathbf{v}_{i+1} + (\sin\gamma_i)\mathbf{S}(\mathbf{w}_i)\mathbf{v}_{i+1}.$$

Since $\mathbf{v}_{i+1}$ is perpendicular to $\mathbf{w}_i$, $\mathbf{r}_i$ can be simplified as

$$\begin{aligned} \mathbf{r}_i &= (\cos\gamma_i)\mathbf{v}_{i+1} + (\sin\gamma_i)\mathbf{S}(\mathbf{w}_i)\mathbf{v}_{i+1} \\ &= [a_i \quad b_i \quad c_i]^T \quad \text{for } i = 1, 2, 3 \end{aligned} \tag{5}$$

where w_{ix}, w_{iy}, and w_{iz} are the Cartesian components of the unit vector $\mathbf{w}_i$ and $\mathbf{S}(\mathbf{w}_1)$ is a skew-symmetric matrix. Also, a_i, b_i, and c_i are the components of the unit vector $\mathbf{r}_i$ in Cartesian coordinate. For simplicity, and without loss of generality, we assume that the unit vectors $\mathbf{v}_2$ and $\mathbf{v}_3$ are in the X–Y plane. Therefore,

$$\mathbf{w}_1 = [0 \quad 0 \quad 1]^{\mathrm{T}}, \quad \mathbf{r}_1 = [a_1 \quad b_1 \quad 0]^{\mathrm{T}}. \tag{6}$$

The unit vector $\mathbf{t}_1$ can now be obtained by rotating the unit vector $\mathbf{w}_1$ about the unit vector $\mathbf{r}_1$ by negative θ_1 angle. Note that θ_1 is also the revolution of passive revolute joint. Since $\mathbf{w}_1$ is perpendicular to $\mathbf{r}_1$, $\mathbf{t}_1$ can be simplified as

$$\mathbf{t}_1 = \mathbf{Q}(\mathbf{r}_1, -\theta_1)\mathbf{w}_1 = (\cos\theta_1)\mathbf{w}_1 - (\sin\theta_1)\mathbf{S}(\mathbf{r}_1)\mathbf{w}_1 \tag{7}$$

where $\mathbf{S}(\mathbf{r}_1)$ is a skew-symmetric matrix. Now we can obtain the unit vector **s** by rotating the unit vector $\mathbf{r}_1$ about the unit vector $\mathbf{t}_1$ by negative β_1 angle. Note that β_1 is the equivalent revolution of the passive prismatic joint. Since $\mathbf{t}_1$ is perpendicular to $\mathbf{r}_1$, **s** can be simplified as

$$\mathbf{s} = \mathbf{Q}(\mathbf{t}_1, -\beta_1)\mathbf{r}_1 = (\cos\beta_1)\mathbf{r}_1 - (\sin\beta_1)\mathbf{S}(\mathbf{t}_1)\mathbf{r}_1 \tag{8}$$

where $\mathbf{S}(\mathbf{t}_1)$ is a skew-symmetric matrix. The steps taken thus far have defined, $\mathbf{w}_1$, information about the fixed base, γ_1 angle, the revolution of actuated joint, θ_1 angle, the revolution of the revolute passive joint, and β_1 angle, the equivalent revolution of the passive prismatic joint. This information will help to define, **s**, which is end-effector orientation. The unit vector **s** is a function of θ_1 and β_1 angles. Therefore, for solving forward position problem of the spherical ST manipulator, we must obtain θ_1 and β_1 angles. These two angles are obtained by simultaneously solving two trigonometric equations. The next step of the

https://doi.org/10.1017/S0263574708005031 Published online by Cambridge University Press

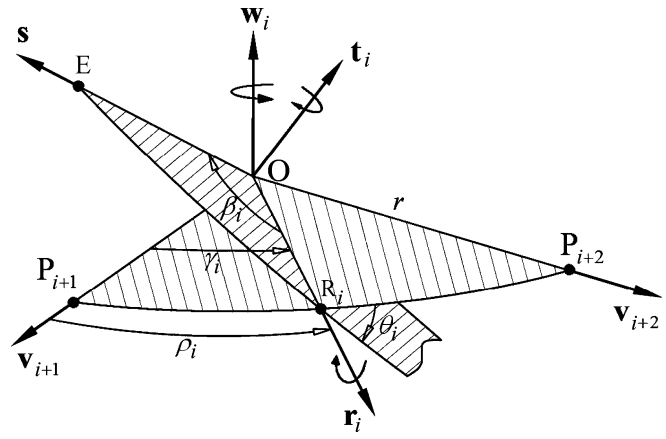

Fig. 3. Geometric model of SST.

solution will utilize the structure of the moveable star in order to find the two trigonometric equations. According to Eq. (3) and Fig. 3, the unit vector, $\mathbf{t}_i$, is perpendicular to the plane that contains the corresponding arc of the moveable star. We previously obtained $\mathbf{t}_1$ as a function of θ_1 and $\mathbf{s}$ as a function of θ_1 and β_1. The unit vectors $\mathbf{t}_2$ and $\mathbf{t}_3$ can now be obtained by rotating $\mathbf{t}_1$ about $\mathbf{s}$ by α_3 and $-\alpha_2$, respectively. Note that $\mathbf{t}_2$ and $\mathbf{t}_3$ are functions of the unknowns θ_1 and β_1

$$\mathbf{t}_2 = \mathbf{Q}(\mathbf{s}, \alpha_3)\mathbf{t}_1 = (\cos\alpha_3)\mathbf{t}_1 + (1-\cos\alpha_3)\mathbf{s}\mathbf{s}^{\mathrm{T}}\mathbf{t}_1 + (\sin\alpha_3)\mathbf{S}(\mathbf{s})\mathbf{t}_1 \tag{9}$$

$$\mathbf{t}_3 = \mathbf{Q}(\mathbf{s}, -\alpha_2)\mathbf{t}_1 = (\cos\alpha_2)\mathbf{t}_1 + (1-\cos\alpha_2)\mathbf{s}\mathbf{s}^{\mathrm{T}}\mathbf{t}_1 - (\sin\alpha_2)\mathbf{S}(\mathbf{s})\mathbf{t}_1 \tag{10}$$

where $\mathbf{S}(\mathbf{s})$ is a skew-symmetric matrix, the unit vector $\mathbf{s}$ is axis of rotation and s_x, s_y, and s_z are its Cartesian components. The unit vector $\mathbf{t}_1$ is perpendicular to the unit vector $\mathbf{s}$. Therefore, Eqs. (9) and (10) can be simplified as

$$\mathbf{t}_2 = (\cos\alpha_3)\mathbf{t}_1 + (\sin\alpha_3)\mathbf{S}(\mathbf{s})\mathbf{t}_1, \tag{11}$$

$$\mathbf{t}_3 = (\cos\alpha_2)\mathbf{t}_1 - (\sin\alpha_2)\mathbf{S}(\mathbf{s})\mathbf{t}_1. \tag{12}$$

The two trigonometric equations are formulated by noting that $\mathbf{t}_2$ is perpendicular to $\mathbf{r}_2$, and $\mathbf{t}_3$ is perpendicular to $\mathbf{r}_3$. Therefore, upon multiplication of both sides of Eqs. (11) and (12) by $\mathbf{r}_2^{\mathrm{T}}$ and $\mathbf{r}_3^{\mathrm{T}}$, respectively, we get

$$\mathbf{r}_2^{\mathrm{T}}\mathbf{t}_2 = (\cos\alpha_3)\mathbf{r}_2^{\mathrm{T}}\mathbf{t}_1 + (\sin\alpha_3)\mathbf{r}_2^{\mathrm{T}}\mathbf{S}(\mathbf{s})\mathbf{t}_1 = 0, \tag{13}$$

$$\mathbf{r}_3^{\mathrm{T}}\mathbf{t}_3 = (\cos\alpha_2)\mathbf{r}_3^{\mathrm{T}}\mathbf{t}_1 - (\sin\alpha_2)\mathbf{r}_3^{\mathrm{T}}\mathbf{S}(\mathbf{s})\mathbf{t}_1 = 0. \tag{14}$$

Next, we substitute the kinematic parameters of the spherical ST parallel manipulator into Eqs. (13) and (14) and rewrite them as

$$d_1\sin\beta_1 + d_2\cos\beta_1 + d_3 = 0 \tag{15}$$

$$d_4\sin\beta_1 + d_5\cos\beta_1 + d_6 = 0 \tag{16}$$

where

$$d_1 = -(a_1a_2 + b_1b_2)\sin\alpha_3 \tag{17(a)}$$

$$d_2 = -\sin\alpha_3[-c_2\sin\theta_1 + (a_1b_2 - b_1a_2)\cos\theta_1] \tag{17(b)}$$

$$d_3 = \cos\alpha_3[(a_1b_2 - b_1a_2)\sin\theta_1 + c_2\cos\theta_1] \tag{17(c)}$$

$$d_4 = (a_1a_3 + b_1b_3)\sin\alpha_1 \tag{17(d)}$$

$$d_5 = \sin\alpha_1[-c_3\sin\theta_1 + (a_1b_3 - b_1a_3)\cos\theta_1] \tag{17(e)}$$

$$d_6 = \cos\alpha_1[(a_1b_3 - b_1a_3)\sin\theta_1 + c_3\cos\theta_1] \tag{17(f)}$$

4. Bezout's Elimination Method

Bezout's elimination method is traditionally used for reducing a set of polynomials of multiple variables into a polynomial of only one variable. To apply Bezout's elimination method to solve the nonlinear Eqs. (15) and (16), the trigonometric equations must be transformed into a set of polynomials. This transformation can be achieved by using the following trigonometric identities:

$$\sin\beta_1 = \frac{2x_1}{1+x_1^2}, \quad \cos\beta_1 = \frac{1-x_1^2}{1+x_1^2} \quad \text{and}$$
$$\sin\theta_1 = \frac{2x_2}{1+x_2^2}, \quad \cos\theta_1 = \frac{1-x_2^2}{1+x_2^2} \tag{18}$$

where $x_1 = \tan(\beta_1/2)$ and $x_2 = \tan(\theta_1/2)$. Next, Eq. (18) is placed into Eqs. (15) and (16). This step is performed using MAPLE software. Results are manually organized into Eqs. (19) and (20) which can then be used by Bezout's elimination method.

$$\left(F_1x_2^2 + F_2x_2 - F_1\right)x_1^2 + \left(F_4x_2^2 + F_4\right)x_1 + \left(F_5x_2^2 + F_3x_2 - F_5\right) = 0 \tag{19}$$

$$\left(F_6x_2^2 + F_7x_2 - F_6\right)x_1^2 + \left(F_9x_2^2 + F_9\right)x_1 + \left(F_{10}x_2^2 + F_8x_2 - F_{10}\right) = 0 \tag{20}$$

where

$$\begin{aligned} &F_1 = J_2 - J_4, \quad F_2 = 2(J_3 - J_1), \quad F_3 = 2(J_1 + J_3),\\ &F_4 = 2d_1, \quad F_5 = -(J_2 + J_4),\\ &F_6 = J_6 - J_8, \quad F_7 = 2(J_7 - J_5),\\ &F_8 = 2(J_5 + J_7),\ F_9 = 2d_4, \quad F_{10} = -(J_6 + J_8) \end{aligned} \tag{21}$$

and

$$J_1 = c_2\sin\alpha_3 \tag{22(a)}$$

$$J_2 = (b_1a_2 - a_1b_2)\sin\alpha_3 \tag{22(b)}$$

$$J_3 = (a_1b_2 - b_1a_2)\cos\alpha_3 \tag{22(c)}$$

$$J_4 = c_2\cos\alpha_3 \tag{22(d)}$$

$$J_5 = -c_3\sin\alpha_1 \tag{22(e)}$$

https://doi.org/10.1017/S0263574708005031 Published online by Cambridge University Press

$$J_6 = -(b_1a_3 - a_1b_3)\sin\alpha_1 \qquad (22(f))$$

$$J_7 = (a_1b_3 - b_1a_3)\cos\alpha_1 \qquad (22(g))$$

$$J_8 = c_3\cos\alpha_1. \qquad (22(h))$$

Using Bezout's elimination method we can eliminate the variable x_1 from Eqs. (19) and (20). The resulting equation is given as follows:

$$\begin{vmatrix} \begin{vmatrix} F_1x_2^2+F_2x_2-F_1 & F_5x_2^2+F_3x_2-F_5 \\ F_6x_2^2+F_7x_2-F_6 & F_{10}x_2^2+F_8x_2-F_{10} \end{vmatrix} & \begin{vmatrix} F_4x_2^2+F_4 & F_5x_2^2+F_3x_2-F_5 \\ F_9x_2^2+F_9 & F_{10}x_2^2+F_8x_2-F_{10} \end{vmatrix} \\ \begin{vmatrix} F_1x_2^2+F_2x_2-F_1 & F_4x_2^2+F_4 \\ F_6x_2^2+F_7x_2-F_6 & F_9x_2^2+F_9 \end{vmatrix} & \begin{vmatrix} F_1x_2^2+F_2x_2-F_1 & F_5x_2^2+F_3x_2-F_5 \\ F_6x_2^2+F_7x_2-F_6 & F_{10}x_2^2+F_8x_2-F_{10} \end{vmatrix} \end{vmatrix} = 0 \qquad (23)$$

Therefore, we have the following eighth-order single variable polynomial:

$$N_8x_2^8 + N_7x_2^7 + N_6x_2^6 + N_5x_2^5 + N_4x_2^4 + N_3x_2^3 + N_2x_2^2 + N_1x_2 + N_0 = 0. \qquad (24)$$

The values for N_0 through N_8 are defined in the Appendix.

5. Case Study

In this section, we present two examples for forward position problem of ST spherical parallel manipulator. The first example uses an isotropic structure while the second provides an example for a nonisotropic case. In the forward position problem ρ_i, $\mathbf{v}_i$, and α_i are supplied. These variables represent stroke of actuators, information on fixed base geometry, and information on moveable star geometry. The orientation of the moving spherical star, $\mathbf{s}$, is determined by solving for θ_1 and β_1.

5.1. Example 1: isotropic case

(i) *Architecture parameters—fixed base:* Assume that the planes OP_2P_3, OP_1P_2, and OP_1P_3 of the manipulator locate in X–Y, X–Z, and Y–Z, respectively. Therefore,

$$\mathbf{v}_1 = [0\ 0\ 1\ ]^{\mathrm{T}}, \quad \mathbf{v}_2 = [1\ 0\ 0\ ]^{\mathrm{T}}, \quad \mathbf{v}_3 = [0\ 1\ 0\ ]^{\mathrm{T}}$$

(ii) *Architecture parameters—moveable star platform:* Assume that the angle between the planes OSR_i and OSR_{i+1} is 120°. Therefore,

$$\alpha_1 = \alpha_2 = \alpha_3 = 120^\circ$$

(iii) *Position of the actuators:* Assume that the radius of sphere is unity and stroke of actuators is $\rho_i = \pi/4$. From Eqs. (4) and (5), we can obtain angle of rotation and unit position vector of the prismatic actuators

$$\gamma_i = 45^\circ \quad \text{for} \quad i = 1,\ 2,\ 3$$

$$\mathbf{r}_1 = \left[\frac{\sqrt{2}}{2} \quad \frac{\sqrt{2}}{2} \quad 0\right]^{\mathrm{T}}, \quad \mathbf{r}_2 = \left[0 \quad \frac{\sqrt{2}}{2} \quad \frac{\sqrt{2}}{2}\right]^{\mathrm{T}},$$

$$\mathbf{r}_3 = \left[\frac{\sqrt{2}}{2} \quad 0 \quad \frac{\sqrt{2}}{2}\right]^{\mathrm{T}}.$$

(iv) *Computation of the orientation of the moving spherical star:* We substitute variables from previous steps into Eqs. (21), (22), and (A.1) through (A.9). Therefore, we can write Eq. (24) as

$$-3x_2^8 + 108x_2^6 - 210x_2^4 + 108x_2^2 - 3 = 0.$$

x_2 can now be solved by placing this equation into MAPLE software. θ_1 can then be calculated using Eq. (18). The value for θ_1 is next placed into Eqs. (15) and (16) which results in finding β_1. Results are listed in Table I. This completes the forward position problem. The 8-degree polynomial results in eight real solutions. Therefore, the polynomial in Eq. (24) is optimum which indicates the solution method is also optimum. All eight solutions are shown graphically in Figs. 4–11.

Table I. Solutions for isotropic example.

Solution	x_2	θ_1	β_1
1	1	90°	35.26438968°
2	−1	−90°	144.7356103°
3	$3-2\sqrt{2}$	19.47122063°	215.2643897°
4	$3+2\sqrt{2}$	(180 − 19.47122063)°	215.2643897°
5	$-3-2\sqrt{2}$	(180 + 19.47122063)°	144.7356103°
6	$-3+2\sqrt{2}$	−19.47122063°	144.7356103°
7	1	90°	215.2643897°
8	−1	−90°	324.7356103°

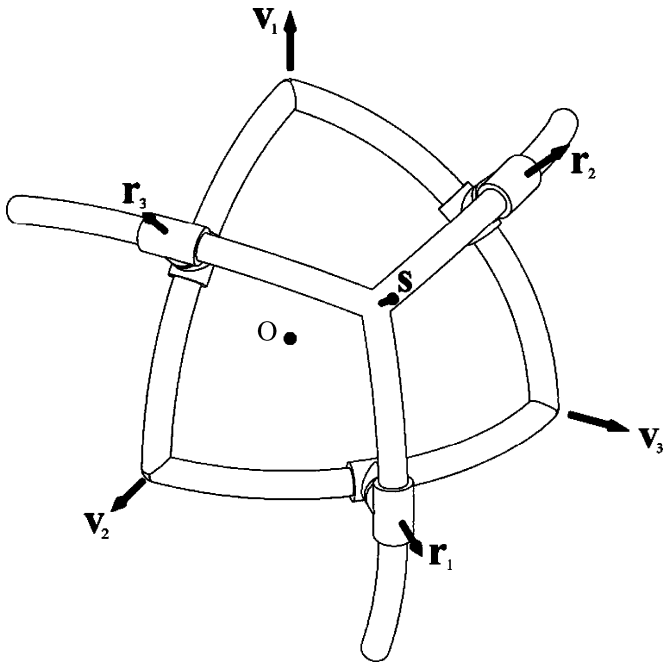

Fig. 4. Solution 1 of isotropic SST.

https://doi.org/10.1017/S0263574708005031 Published online by Cambridge University Press

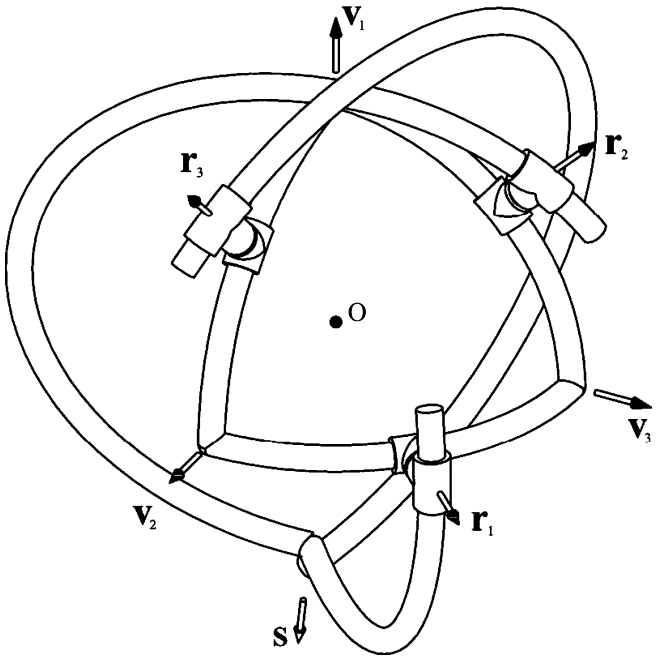

Fig. 5. Solution 2 of isotropic SST.

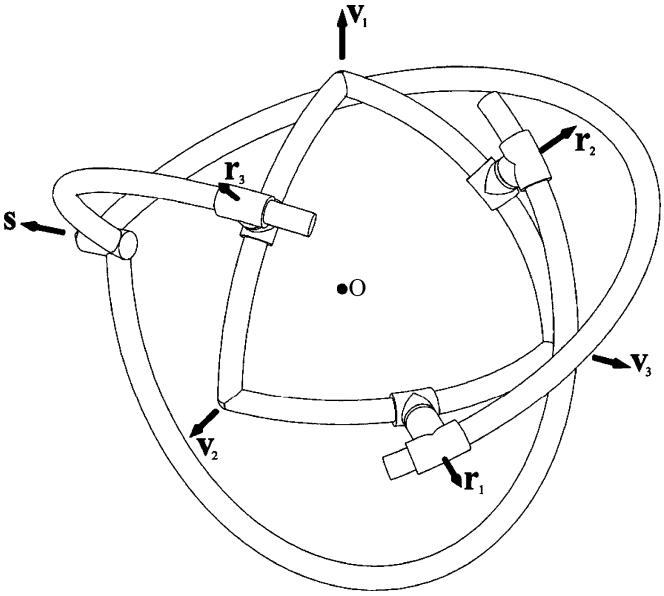

Fig. 7. Solution 4 of isotropic SST.

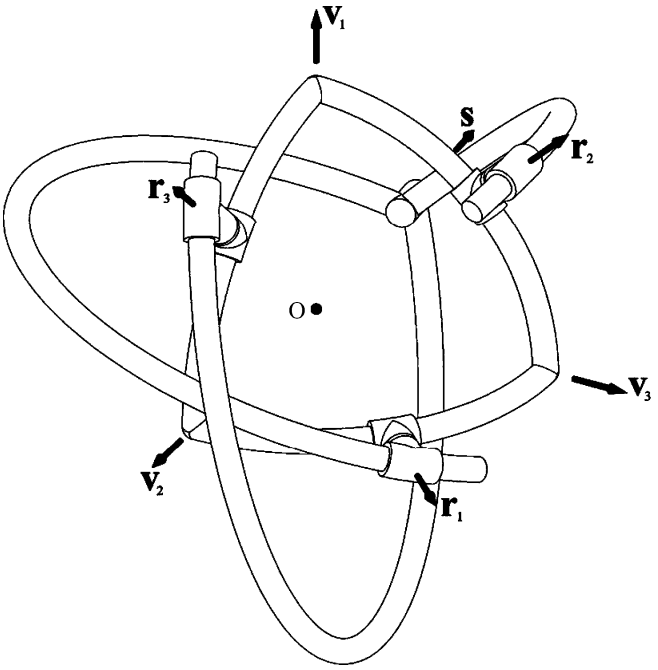

Fig. 6. Solution 3 of isotropic SST.

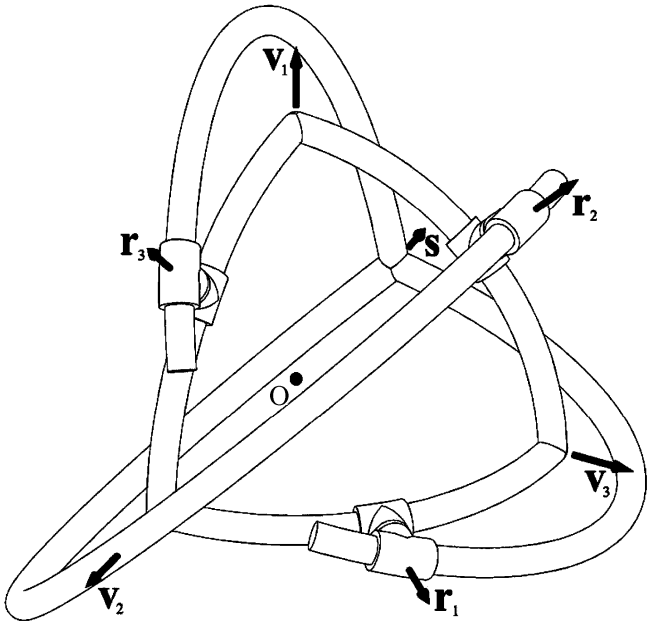

Fig. 8. Solution 5 of isotropic SST.

5.2. Example 2: nonisotropic case

(i) *Architecture parameters—fixed base*

$$\mathbf{v}_1 = [0 \quad 0 \quad 1]^{\mathrm{T}}, \quad \mathbf{v}_2 = [0 \quad 1 \quad 0]^{\mathrm{T}},$$
$$\mathbf{v}_3 = [\sqrt{2}/4 \quad \sqrt{2}/4 \quad \sqrt{3}/2]^{\mathrm{T}}$$

(ii) *Architecture parameters—moveable star platform*

$$\alpha_1 = \alpha_2 = \alpha_3 = 120^\circ$$

(iii) *Position of the actuators.* Assume that the radius of sphere is unity and stroke of actuators are $\rho_1 = \pi/4$ and $\rho_2 = \rho_2 = \pi/6$. From Eqs. (4) and (5) we can obtain angle of rotation and unit position vector of the prismatic actuators

$$\gamma_1 = 45^\circ \quad \text{and} \quad \gamma_2 = \gamma_2 = 30^\circ$$
$$\mathbf{r}_1 = \left[\frac{\sqrt{2}}{2} \quad \frac{\sqrt{2}}{2} \quad 0\right]^{\mathrm{T}}, \quad \mathbf{r}_2 = \left[\frac{\sqrt{7}}{14} \quad \frac{\sqrt{3}}{2} \quad \frac{\sqrt{42}}{14}\right]^{\mathrm{T}},$$
$$\mathbf{r}_3 = \left[\frac{\sqrt{6}+\sqrt{14}}{8} \quad \frac{7\sqrt{6}-\sqrt{14}}{56} \quad \frac{21-\sqrt{21}}{28}\right]^{\mathrm{T}}.$$

(iv) *Computation of the orientation of the moving spherical star.* Substituting variables from previous steps into

https://doi.org/10.1017/S0263574708005031 Published online by Cambridge University Press

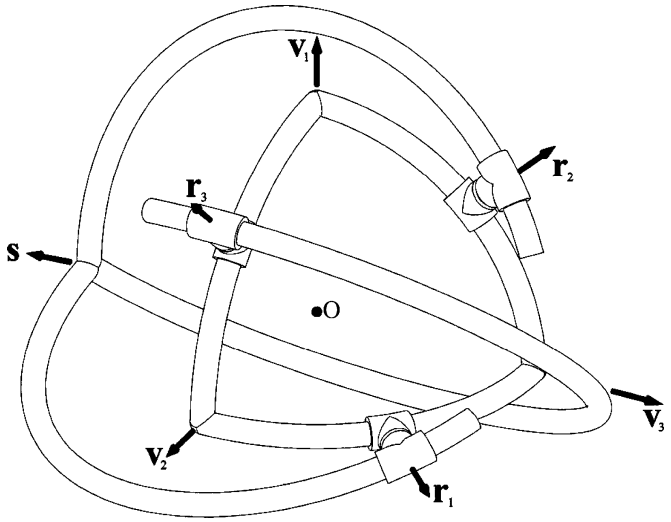

Fig. 9. Solution 6 of isotropic SST.

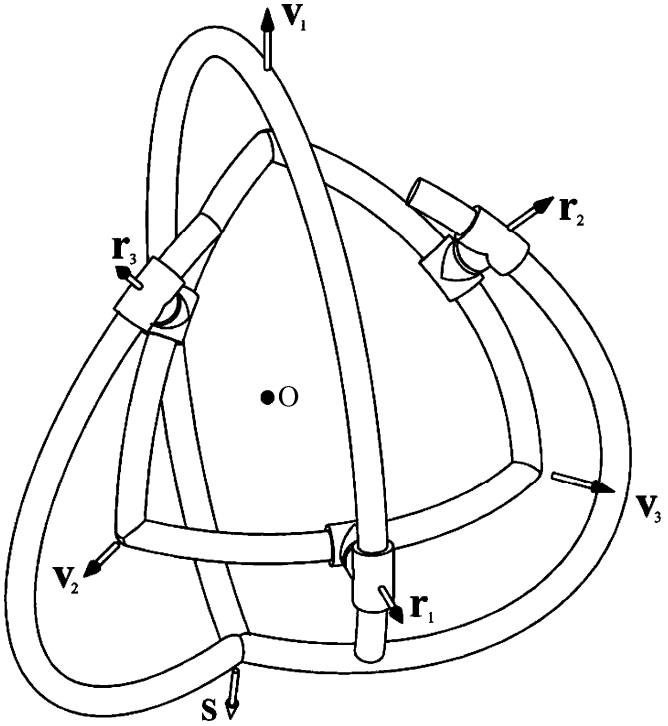

Fig. 10. Solution 7 of isotropic SST.

Eqs. (21), (22), and (A.1) through (A.9) will allow us to write Eq. (24) as

$$
\begin{aligned}
&(486\sqrt{21}+450)x_2^8-(4176\sqrt{7}-3696\sqrt{3})x_2^7\\
&\quad-(12,120+456\sqrt{21})x_2^6+(18,864\sqrt{7}-23,\\
&\quad\times 184\sqrt{3})x_2^5+(40,140-3420\sqrt{21})x_2^4\\
&\quad-(18,864\sqrt{7}-23,184\sqrt{3})x_2^3\\
&\quad-(12,120+456\sqrt{21})x_2^2+(4176\sqrt{7}\\
&\quad+3696\sqrt{3})x_2+(486\sqrt{21}+450)=0
\end{aligned}
$$

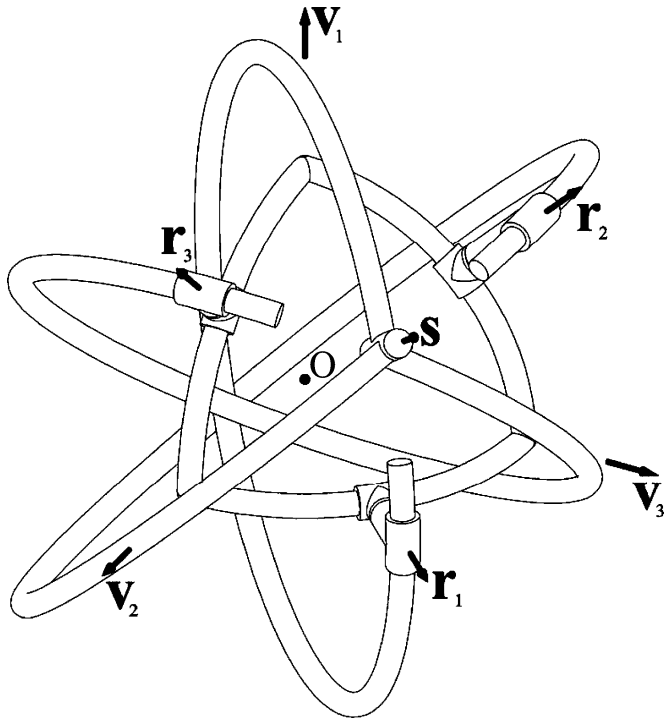

Fig. 11. Solution 8 of isotropic SST.

Table II. Real solutions for nonisotropic example.

Solution	x_2	θ_1	β_1
1	1.139057012	97.43896455°	19.67101001°
2	2.834997880	141.14104776°	(180 + 39.64623229)°
3	−0.3527339498	−38.85895224°	(180 − 39.64623229)°
4	−0.8779191815	−82.56103545°	(360 − 19.67101001)°

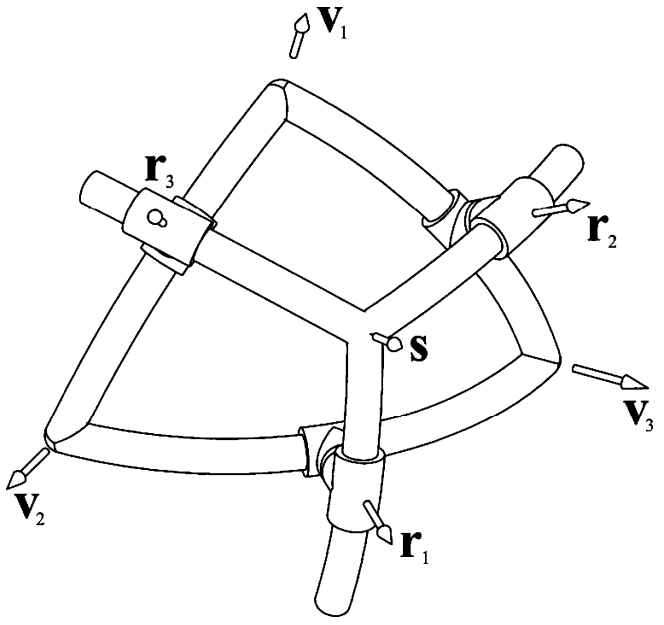

Fig. 12. Solution 1 of nonisotropic SST.

For this equation eight solutions are found, however, only four are real. Results are listed in Table II. All four solutions are also shown graphically in Figs. 12–15.

https://doi.org/10.1017/S0263574708005031 Published online by Cambridge University Press

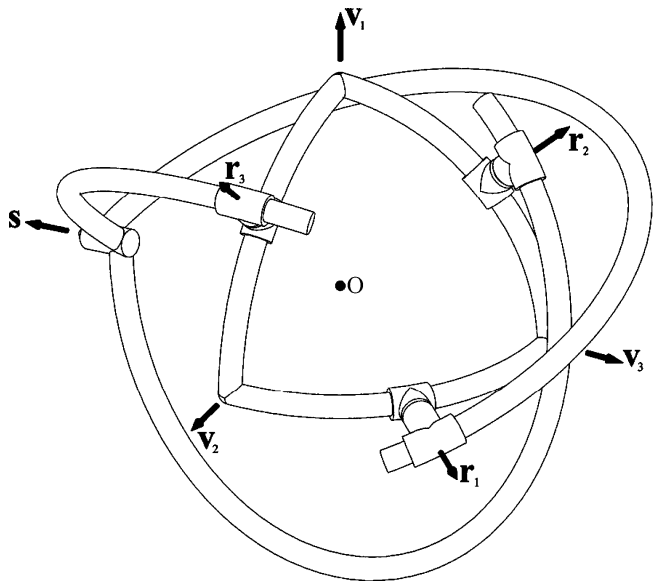

Fig. 13. Solution 2 of nonisotropic SST.

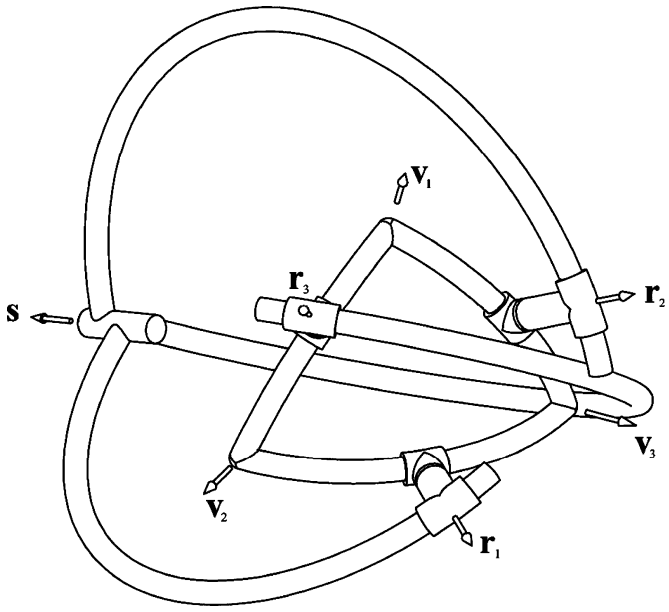

Fig. 14. Solution 3 of nonisotropic SST.

6. Jacobian Matrices

The differential kinematic relations pertaining to parallel manipulators take the form

$$\mathbf{J}\dot{\boldsymbol{\gamma}} + K\boldsymbol{\omega} = 0 \tag{25}$$

where $\mathbf{J}$ and $\mathbf{K}$ are the two Jacobian matrices for the manipulator at hand. Moreover, $\dot{\boldsymbol{\gamma}}$ is the vector of joint rates and $\boldsymbol{\omega}$ is the twist array. The angular velocity $\boldsymbol{\omega}$ of the end-effector can now be written as

$$\mathbf{w}_i\dot{\gamma}_i - \mathbf{r}_i\dot{\theta}_i - \mathbf{t}_i\dot{\beta}_i = \boldsymbol{\omega}, \quad i = 1,\ 2,\ 3 \tag{26}$$

where θ_i is the angle between planes OR $_i$S and OP$_{i+1}$P$_{i+2}$, while β_i is the angle between $\mathbf{s}$ and $\mathbf{r}_i$. Note that β_i is equivalent revolution of the passive prismatic joint and θ_i is revolution of the passive revolute joint. Furthermore, we have

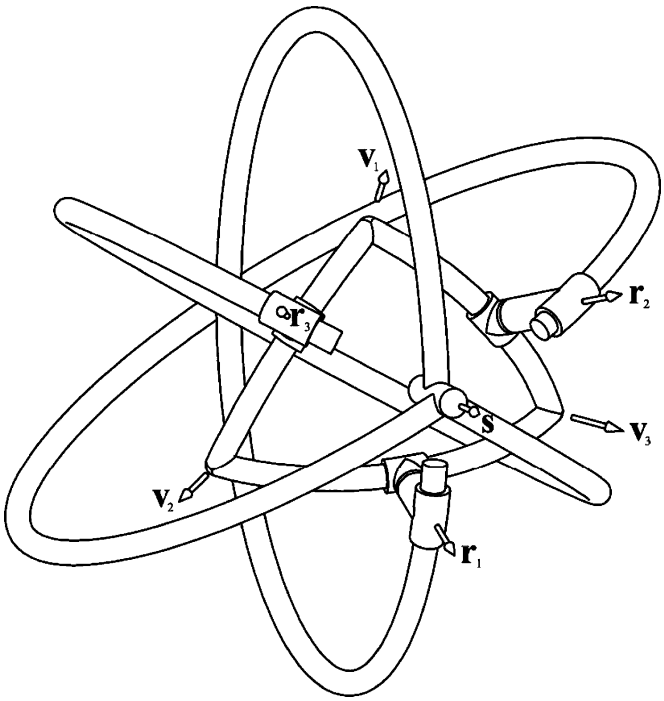

Fig. 15. Solution 4 of nonisotropic SST.

$$\dot{\gamma}_i = \dot{\rho}_i/\mathbf{r}, \quad i = 1, 2, 3. \tag{27}$$

The inner product of both sides of Eq. (26) with $\mathbf{r}_i \times \mathbf{t}_i$ leads to an equation free of passive joints rates, which simplifies to

$$(\mathbf{r}_i \times \mathbf{t}_i)\cdot\mathbf{w}_i\dot{\gamma}_i - (\mathbf{r}_i \times \mathbf{t}_i)\cdot\boldsymbol{\omega} = 0, \quad i = 1, 2, 3. \tag{28}$$

Equations (26)–(28), for $i = 1, 2, 3$, are now combined and expressed in vector form as Eq. (25). Therefore, we can define $\mathbf{J}$ and $\mathbf{K}$ as

$$\mathbf{J} = \begin{bmatrix} c_1 & 0 & 0 \\ 0 & c_2 & 0 \\ 0 & 0 & c_3 \end{bmatrix} \tag{29}$$

and

$$\mathbf{K} = \begin{bmatrix} -(\mathbf{r}_1 \times \mathbf{t}_1)^{\mathrm{T}} \\ -(\mathbf{r}_2 \times \mathbf{t}_2)^{\mathrm{T}} \\ -(\mathbf{r}_3 \times \mathbf{t}_3)^{\mathrm{T}} \end{bmatrix} \tag{30}$$

in which

$$c_i = (\mathbf{r}_i \times \mathbf{t}_i)^{\mathrm{T}}\mathbf{w}_i. \tag{31}$$

7. Acceleration Analysis

In this section, we relate the angular acceleration of the moving spherical star to the accelerations of actuators. By taking derivative of Eq. (26) the angular acceleration of the

https://doi.org/10.1017/S0263574708005031 Published online by Cambridge University Press

moving spherical star can be written as

$$\mathbf{w}_i\ddot{\gamma}_i + \dot{\mathbf{w}}_i\dot{\gamma}_i - \mathbf{r}_i\ddot{\theta}_i - \dot{\mathbf{r}}_i\dot{\theta}_i - \mathbf{t}_i\ddot{\beta}_i - \dot{\mathbf{t}}_i\dot{\beta}_i = \dot{\boldsymbol{\omega}}, \quad i = 1, 2, 3. \tag{32}$$

From Figs. 2 and 3, the derivatives of the three unit vectors may be written as

$$\dot{\mathbf{w}}_i = \mathbf{0} \tag{33}$$

$$\dot{\mathbf{r}}_i = \dot{\gamma}_i\mathbf{w}_i \times \mathbf{r}_i \tag{34}$$

$$\dot{\mathbf{t}}_i = (\dot{\gamma}_i\mathbf{w}_i - \dot{\theta}_i\mathbf{r}_i) \times \mathbf{t}_i \tag{35}$$

By putting Eqs. (33)–(35) into Eq. (32) and using Eq. (26), the angular acceleration of the moving spherical star for the ith leg can be written as

$$\mathbf{w}_i\ddot{\gamma}_i - \mathbf{r}_i\ddot{\theta}_i - \dot{\gamma}_i\dot{\theta}_i(\mathbf{w}_i \times \mathbf{r}_i) - \mathbf{t}_i\ddot{\beta}_i - \dot{\beta}_i(\boldsymbol{\omega} \times \mathbf{t}_i) = \dot{\boldsymbol{\omega}} \tag{36}$$

where $\ddot{\gamma}_i$ is the angular acceleration of the actuators, $\ddot{\theta}_i$ is the angular acceleration of the passive revolute joint, $\ddot{\beta}_i$ is the equivalent angular acceleration for the passive prismatic joint, and $\dot{\boldsymbol{\omega}}$ is the angular acceleration of the moving spherical star.

Upon multiplication of the two sides of Eq. (36) by $(\mathbf{r}_i \times \mathbf{t}_i)^{\mathrm{T}}$ and eliminating angular acceleration of the passive joints $\ddot{\theta}_i$ and $\ddot{\beta}_i$, Eq. (36) can be rewritten as

$$\begin{aligned} c_i\ddot{\gamma}_i &- (\mathbf{r}_i \times \mathbf{t}_i)\cdot\dot{\boldsymbol{\omega}} + \dot{\gamma}_i\dot{\theta}_i(\mathbf{r}_i \times \mathbf{t}_i)\cdot(\mathbf{w}_i \times \mathbf{r}_i) \\ &- \dot{\gamma}_i\dot{\beta}_i(\mathbf{r}_i \times \mathbf{t}_i)\cdot(\mathbf{w}_i \times \mathbf{t}_i) + \dot{\theta}_i\dot{\beta}_i = 0. \end{aligned} \tag{37}$$

Using Eq. (26), we can obtain the angular velocity of the passive joints $\dot{\theta}_i$ and $\dot{\beta}_i$. For this purpose, we multiply the two sides of Eq. (26) by $(\mathbf{r}_i)^{\mathrm{T}}$ and $(\mathbf{t}_i)^{\mathrm{T}}$, separately. Since the unit vector $\mathbf{r}_i$ is perpendicular to the unit vectors $\mathbf{w}_i$ and $\mathbf{t}_i$ both, we can obtain $\dot{\theta}_i$ and $\dot{\beta}_i$ as follows:

$$\dot{\theta}_i = -(\mathbf{r}_i)^{\mathrm{T}}\boldsymbol{\omega} \tag{38}$$

$$\dot{\beta}_i = \dot{\gamma}_i(\mathbf{t}_i)^{\mathrm{T}}\mathbf{w}_i - (\mathbf{t}_i)^{\mathrm{T}}\boldsymbol{\omega}. \tag{39}$$

Substituting these values into Eq. (37) and simplifying will lead to

$$\begin{aligned} c_i\ddot{\gamma}_i &- (\mathbf{r}_i \times \mathbf{t}_i)\cdot\dot{\boldsymbol{\omega}} - 2\dot{\gamma}_i(\mathbf{r}_i\cdot\boldsymbol{\omega})(\mathbf{t}_i\cdot\mathbf{w}_i) \\ &+ (\mathbf{r}_i\cdot\boldsymbol{\omega})(\mathbf{t}_i\cdot\boldsymbol{\omega}) = 0. \end{aligned} \tag{40}$$

For $i = 1, 2, 3$, thisequation can be written in the matrix form as

$$\mathbf{J}\ddot{\boldsymbol{\gamma}} + \mathbf{K}\dot{\boldsymbol{\omega}} + \mathbf{M}\dot{\boldsymbol{\gamma}} + \mathbf{N} = \mathbf{0} \tag{41}$$

in which matrices $\mathbf{J}$ and $\mathbf{K}$ were defined earlier and matrices $\mathbf{M}$ and $\mathbf{N}$ are defined as

$$\mathbf{M} = \begin{bmatrix} d_1 & 0 & 0 \\ 0 & d_2 & 0 \\ 0 & 0 & d_3 \end{bmatrix} \tag{42}$$

$$\mathbf{N} = \begin{bmatrix} e_1 & 0 & 0 \\ 0 & e_2 & 0 \\ 0 & 0 & e_3 \end{bmatrix} \tag{43}$$

where

$$d_i = (\mathbf{r}_i\cdot\boldsymbol{\omega})(\mathbf{t}_i\cdot\mathbf{w}_i), \quad e_i = (\mathbf{r}_i\cdot\boldsymbol{\omega})(\mathbf{t}_i\cdot\boldsymbol{\omega}) \ \text{ for } \ i = 1,\ 2,\ 3 \tag{44}$$

Equation (41) shows the relationship between angular velocity and angular acceleration of the moving spherical star and angular velocity and angular acceleration of the three actuators.

8. Singularity Analysis

In parallel manipulators, singularities occur whenever $\mathbf{J}$, $\mathbf{K}$, or both become singular. Thus, for these manipulators a distinction can be made between three types of singularities which have different kinematic interpretations, namely,

1. The first type of singularity occurs when $\mathbf{J}$ becomes singular but $\mathbf{K}$ is nonsingular, i.e., when $\det(\mathbf{J}) = 0$ and $\det(\mathbf{K}) \neq 0$. This type of singularity consists of a set of points where at least two branches of the inverse kinematics meet. Since the nullity of $\mathbf{J}$ is not zero, we can find a set of nonzero actuator velocity vectors, $\dot{\boldsymbol{\gamma}}$, for which the Cartesian velocity vector $\boldsymbol{\omega}$ is zero. Then, nonzero Cartesian velocity vectors, $K\boldsymbol{\omega}$, those lying in the null space of $\mathbf{J}^{\mathrm{T}}$, cannot be produced. The manipulator thus losing one or more degrees of freedom.
2. The second type of singularity, occurring only in closed kinematic chains, arises when $\mathbf{K}$ becomes singular but $\mathbf{J}$ is non singular, i.e., when $\det(\mathbf{J}) \neq 0$ and $\det(\mathbf{K}) = 0$. This type of singularity consists of a point or a set of points whereby different branches of the direct kinematics problem meet. Since the nullity of $\mathbf{K}$ is not zero, we can find a set of nonzero Cartesian velocity vectors, $\boldsymbol{\omega}$, for which the actuator velocity vector, $\dot{\boldsymbol{\gamma}}$, is zero. Then, the mechanism gains one or more degrees of freedom or equivalently, cannot resist forces or moments in one or more directions, even if all the actuators are locked.
3. The third type of singularity occurs when both $\mathbf{J}$ and $\mathbf{K}$ are simultaneously singular while none of the rows of $\mathbf{K}$ vanishes. Under a singularity of this type, configurations arise for which moving platform can undergo finite motions even if the actuators are locked or equivalently, it cannot resist forces or moments in one or more directions over a finite portion of the workspace, even if all the actuators are locked. As well, a finite motion of the actuators produces no motion of moveable platform and some of the Cartesian velocity vectors cannot be produced. This type of singularity is shown in Fig. 19.

8.1. Singularity analysis of spherical ST manipulator

In this subsection, the three singularity types are investigated for the manipulator of Fig. 1.

1. The first type of singularity occurs when the determinant of $\mathbf{J}$ vanishes. From Eqs. (29) and (31), this condition

https://doi.org/10.1017/S0263574708005031 Published online by Cambridge University Press

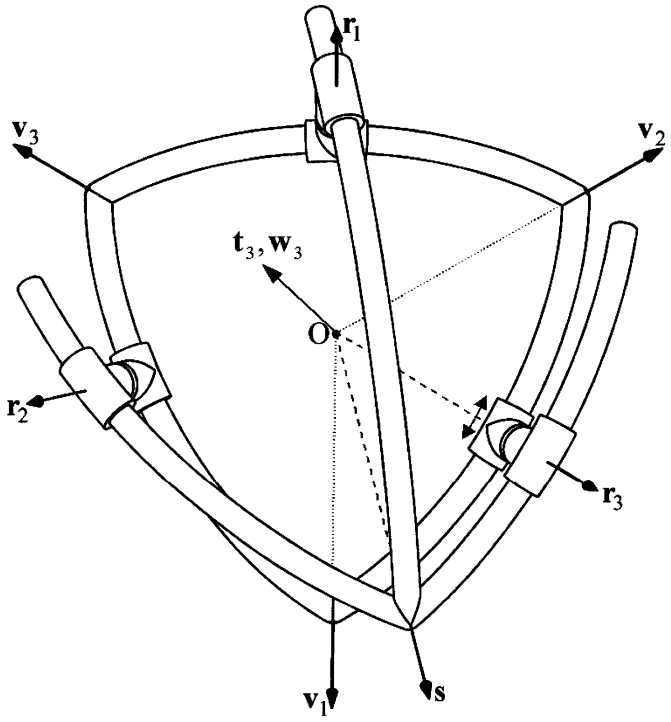

Fig. 16. First type singularity of SST.

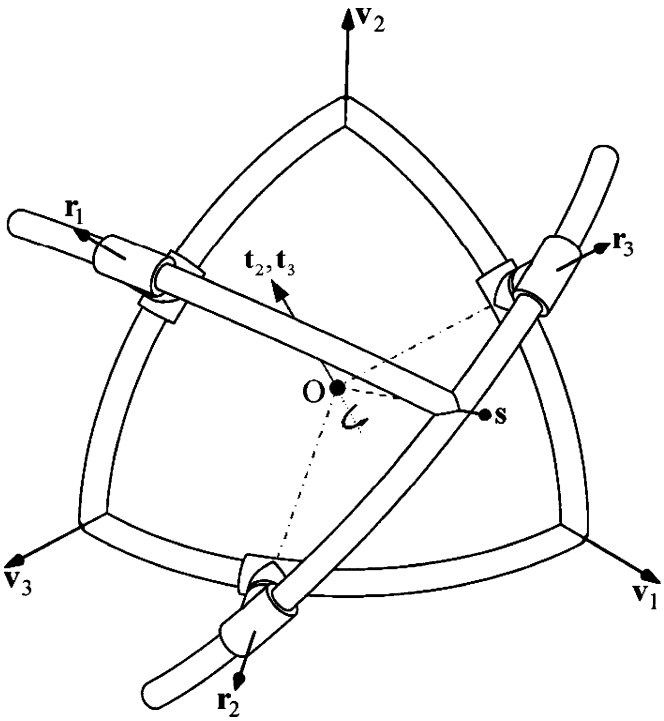

Fig. 17. Second type singularity of SST.

yields

$$(\mathbf{r}_i \times \mathbf{t}_i) \cdot \mathbf{w}_i = 0 \quad \text{for } i = 1 \text{ or } 2 \text{ or } 3. \tag{45}$$

This type of configuration is reached whenever $\mathbf{w}_i$ is perpendicular to $\mathbf{r}_i \times \mathbf{t}_i$, but $\mathbf{r}_i$ lies in the plane whose normal is $\mathbf{w}_i$, as shown in Fig. 3. Therefore, this type of singularity occurs whenever $\mathbf{w}_i$ and $\mathbf{t}_i$ coincide as shown in Fig. 16. In other words, one of the arcs of the moveable spherical star and one of the arcs of the fixed triangle lie on a single plane that also passes through center of sphere. In this case, the actuator along $\mathbf{w}_i$ does not produce any Cartesian velocity. Thus, the manipulator loses 1-dof.

2. The second type of singularity occurs when the determinant of **K** vanishes, which occurs when the rows or columns of **K** are linearly dependent. By inspection of Eq. (30), we can say that this condition occurs when
   (a) Two rows of **K** are linearly dependent. Therefore, according to Eq. (30), this type of singularity occurs when the two arcs of moveable spherical star turn into one single arc. In other words, the two arcs lie on a single plane that also passes through center of sphere. Therefore, any moment which is perpendicular to this plane and also passes through center of sphere cannot be resisted even if all the actuators are locked. This is shown in Fig. 17.
   (b) One row of **K** is the linear combination of the other two. In this case, the three planes containing $\mathbf{r}_i \times \mathbf{t}_i$ vectors intersect at a common line. But, according to the moveable star architecture of the manipulator, this condition cannot occur.
3. The third type of singularity occurs when the determinants of **J** and **K** both vanish, while none of the rows of **K** vanishes. We have this type of singularity whenever the previously defined two singularities occur simultaneously and $\mathbf{k}_i \neq \mathbf{0}$, where $\mathbf{k}_i^{\mathrm{T}}$, for $i = 1$–3, is the ith row of **K**. The manipulator is then configured as in Fig. 18. In this case, one of the arcs of the moveable spherical star and one of the arcs of the fixed triangle lie on a single plane that also passes through the center of sphere. Therefore, the motion of at least one actuator does not produce any Cartesian velocity. Additionally, the two arcs of moveable spherical star lie on a single plane that also passes through center of sphere. Therefore, any moment which is perpendicular to

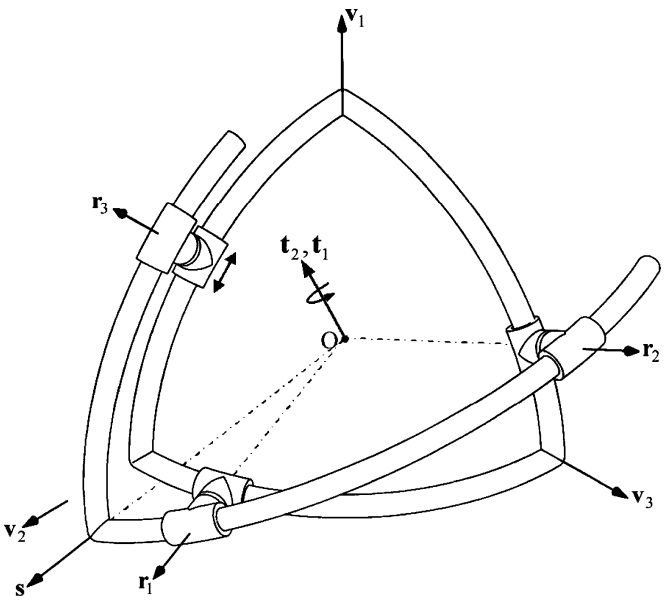

Fig. 18. Third type singularity of SST.

https://doi.org/10.1017/S0263574708005031 Published online by Cambridge University Press

this plane and also passes through center of sphere cannot be resisted even if all the actuators are locked.

9. Isotropic Designs

Mechanism control accuracy depends upon the condition number of the Jacobian matrices **J** and **K**. The condition number is based on a concept common to all matrices, whether square or not, i.e., their singular values. For an $m \times n$ matrix A, with $m < n$, we can define its m singular values as the non-negative square roots of the non-negative eigenvalues of the $m \times n$ matrix $\mathbf{AA^T}$. Because $\mathbf{AA^T}$ is square, symmetric, and at least positive-semidefinite, its eigenvalues are all real and non-negative. Also, if the matrix under investigation is dimensionally homogeneous, then we can meaningfully order the singular values of these matrices from smallest to largest. Thus, if $\sigma_{\min}$ and $\sigma_{\max}$ denote the smallest and the largest singular values of a matrix, its condition number is then defined as

$$\kappa = \frac{\sigma_{\max}}{\sigma_{\min}} \tag{46}$$

and hence, the larger the variance of the singular values, the larger the condition number is. The significance of the condition number of a matrix pertains to the numerical inversion of this matrix while solving a system of linear equations associated with the matrix. Clearly, in the case of nonsquare matrices, this inversion is understood as a generalized inverse. Indeed, when inverting a matrix with finite precision, a roundoff error is always present, and hence, a roundoff error amplification affects the accuracy of the computed results. Furthermore, this amplification is bounded by the condition number of the matrix. It is apparent that a singular matrix has a minimum singular value of zero, and hence, its condition number becomes infinite. Conversely, if the singular values of a matrix are identical, then the condition number of the matrix attains a minimum value of unity. Matrices with such a property are called isotropic. The reason why isotropic matrices are desirable is that they can be inverted at no cost because the inverse of an isotropic matrix or the generalized inverse of a rectangular isotropic matrix for that matter is proportional to its transpose, the proportionality factor being the reciprocal of its multiple singular value.

From the earlier discussion, and considering that the Jacobian matrices are configuration-dependent, it is apparent that the condition number of the Jacobian matrices of a manipulator is configuration-dependent as well, and hence, a manipulator can be designed with an architecture that allows for postures entailing isotropic Jacobian matrices, such a design being called isotropic. However, this property disappears in all other postures. This is a fact of life and nothing can be done about it but one can design for postures that are isotropic and then plan tasks that lie well within a region where the condition number is acceptable. For manipulators with isotropic designs, such regions cover a substantial percentage of the overall workspace. The condition number degenerates only for postures very close to singularities, which should be avoided in trajectory planning, in any event.

9.1. Isotropic design of the spherical ST manipulator

In this subsection, we uncover isotropic designs for the manipulator shown in Fig. 1. Here, we define a design as isotropic if **J** and **K** are both proportional to an identity matrix such that

$$\mathbf{JJ}^T = \sigma^2 \mathbf{I}_{3\times 3}, \tag{47}$$

$$\mathbf{KK}^T = \tau^2 \mathbf{I}_{3\times 3}. \tag{48}$$

Substitution of the expressions of **J** and **K** from Eqs. (29) and (30) into Eqs. (47) and (48) leads to

$$\begin{bmatrix} c_1^2 & 0 & 0 \\ 0 & c_2^2 & 0 \\ 0 & 0 & c_3^2 \end{bmatrix} = \sigma^2 \mathbf{I} \tag{49}$$

$$\begin{bmatrix} \mathbf{d}_1^{\mathrm{T}}\mathbf{d}_1 & \mathbf{d}_1^{\mathrm{T}}\mathbf{d}_2 & \mathbf{d}_1^{\mathrm{T}}\mathbf{d}_3 \\ \mathbf{d}_1^{\mathrm{T}}\mathbf{d}_2 & \mathbf{d}_2^{\mathrm{T}}\mathbf{d}_2 & \mathbf{d}_2^{\mathrm{T}}\mathbf{d}_3 \\ \mathbf{d}_1^{\mathrm{T}}\mathbf{d}_3 & \mathbf{d}_2^{\mathrm{T}}\mathbf{d}_3 & \mathbf{d}_3^{\mathrm{T}}\mathbf{d}_3 \end{bmatrix} = \tau^2 \mathbf{I} \tag{50}$$

where

$$\mathbf{d}_i = \mathbf{r}_i \times \mathbf{t}_i.$$

Equations (49) and (50) give the conditions for isotropy, namely,

$$c_1^2 = c_2^2 = c_3^2 = \sigma^2 \tag{51}$$

$$\mathbf{d}_i^{\mathrm{T}}\mathbf{d}_j = \begin{cases} \tau^2 & \text{if } i = j \\ 0 & \text{if } i \neq j \end{cases}. \tag{52}$$

Using Eqs. (51) and (52) we can obtain

$$\begin{gathered} \angle(\mathbf{s},\mathbf{w}_1) = \angle(\mathbf{s},\mathbf{w}_2) = \angle(\mathbf{s},\mathbf{w}_3) \\ \angle(\mathbf{s},\mathbf{r}_1) = \angle(\mathbf{s},\mathbf{r}_2) = \angle(\mathbf{s},\mathbf{r}_3). \\ \mathbf{r}_1^{\mathrm{T}}\mathbf{r}_2 = \mathbf{r}_1^{\mathrm{T}}\mathbf{r}_3 = \mathbf{r}_2^{\mathrm{T}}\mathbf{r}_3 \end{gathered} \tag{53}$$

Considering the foregoing conditions and the geometry of the problem we find that isotropic designs are only possible if

- The fixed spherical triangle is equilateral or $P_1P_2 = P_1P_3 = P_2P_3$.
- The angles between sides of the moveable spherical star is 120° or $\alpha_1 = \alpha_2 = \alpha_3 = 120^\circ$.
- The end-effector, point E, coincides with geometrical center of the fixed base equilateral triangle.

The one-dimensional continuum of isotropic designs comprises a single variable whose range is given as

$$60^\circ < \alpha_{\mathrm{f}} < 120^\circ.$$

In which α_{f} is an angle that represents the arc of the fixed spherical equilateral triangle. This one-dimensional continuum allows for infinite isotropic structures and enables one to incorporate isotropy as a criterion when designing this type of manipulator. A typical isotropic design of the manipulator is depicted in Fig. 19.

https://doi.org/10.1017/S0263574708005031 Published online by Cambridge University Press

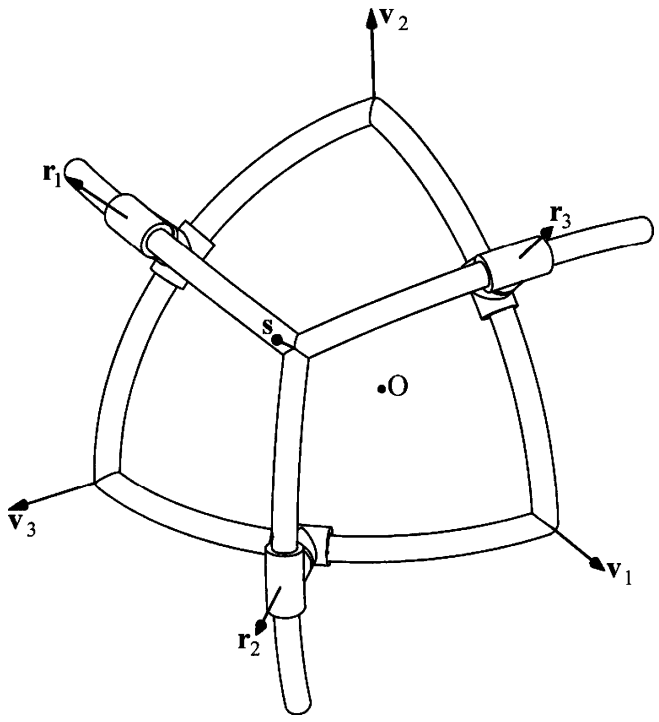

Fig. 19. An isotropic design of SST.

10. Workspace and Accuracy

For workspace analysis, we will assume $\alpha_f = 90^\circ$ and $\alpha_1 = \alpha_2 = \alpha_3 = 120^\circ$ which represents an isotropic design. We will also assume the radius of the sphere as 1 m and will obtain workspace of the manipulator. The workspace depends on the angle θ_1 (see Fig. 3). Therefore, workspace of the manipulator versus angle θ_1 is shown in Fig. 20. It is apparent that maximum workspace occurs at $\theta_1 = 90^\circ$. In this configuration, value of workspace is equal to 1.57 m^2. This value represents one-eighth area of a sphere with radius 1 m. Our earlier selection of $\alpha_f = 90^\circ$ also results in an area for the fixed base triangle equal to 1.57 m^2. Because these two areas are equal, we have shown that the moving spherical star can travel the entire area of its fixed base. Therefore, in its isotropic design the end-effector, **s**, can be positioned anywhere within the surface of the fixed spherical triangular base. Therefore, this shows that the spherical ST manipulator has a relatively large workspace.

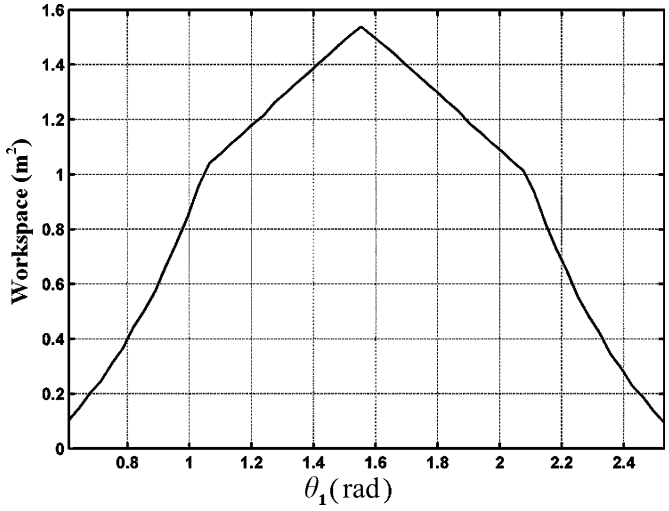

Fig. 20. Workspace of the isotropic design vs. angle θ_1.

Table III. Comparison of GCI values for few parallel manipulators.

Spherical-star triangle	Spherical 3-RRR	Spatial 3-RPS	Planar 3-RRR	Planar 3-RPR
0.67	0.52	0.58	0.79	0.49

Additionally, all points in the workspace are free of singularities. To prove this point we note that singularity requires

1. one of the $\alpha_i = 180^\circ$ and/or
2. one of the arcs of the moveable spherical star and one of the arcs of the fixed triangle lie on a single plane that also passes through center of sphere.

Isotropic design requires $\alpha_1 = \alpha_2 = \alpha_3 = 120^\circ$. Therefore, the first condition for singularity is not possible. The second singularity condition is also physically not possible due to the structure of the isotropic design.

For accuracy analysis of the manipulator in its workspace, we use the concept of global conditioning index (GCI) introduced by Gosselin[19] as

$$\mathrm{GCI} = \frac{\int_W (1/\kappa)\,\mathrm{dW}}{\int_W \mathrm{dW}}. \tag{54}$$

This index corresponds to the average value of $1/\kappa$ (see Eq. (46)). The value of GCI for the isotropic design of the manipulator is equal to 0.67. In Table III, the value of GCI is compared with the optimum design of few 3-dof parallel manipulators.[18] Clearly the GCI of the proposed spherical ST is in "good" range compared with other 3-dof parallel manipulators.

11. Conclusions

A novel spherical parallel manipulator was introduced. Good accuracy and relatively large workspace free of singularities (in isotropic design) made the manipulator suitable for practical applications. The forward position and acceleration analysis, isotropy design, singularity analysis, workspace, and accuracy analysis were outlined. The forward position problem utilizes a solution method based on the equivalent angle–axis representation. Bezout's elimination method was used to obtain a single variable 8-degree polynomial. Two examples, one for isotropic and the other for nonisotropic design, were supplied. For the isotropic example, the 8-degree polynomial results in eight real solutions. Therefore, the polynomial is optimum which indicates the solution method is also optimum. All eight solutions are also shown graphically. Next, using invariant form, we performed acceleration and singularity analysis. Using the same form, also

https://doi.org/10.1017/S0263574708005031 Published online by Cambridge University Press

we found conditions for singularity and obtained the isotropy design of spherical ST manipulator. It was shown that the spherical ST manipulator has infinite isotropic designs. This allows one the freedom to incorporate design criteria besides isotropy. Using isotropic design and singularity requirements, we showed the workspace of the isotropic spherical ST is free of singularity. Finally, the GCI of the proposed spherical ST was calculated and was shown to be in "good" range compared with other 3-dof parallel manipulators.

References

1. D. Chablat and J. Angeles, "The computation of all 4R serial spherical wrists with an isotropic architecture," *ASME J. Mech. Des.* **125**(2), 275–280 (2003).
2. C. M. Gosselin and J. Angeles, "The optimum kinematics design of a spherical three-degree-of-freedom parallel manipulator," *ASME J. Mech. Des.* **111**(2), 202–207 (1989).
3. C. M. Gosselin, J. Sefrioui and M. J. Richard, "On the direct kinematics of spherical three-degree-of-freedom parallel manipulators of general architecture," *ASME J. Mech. Des.* **116**(2), 594–598 (1994).
4. C. M. Gosselin, L. Perreault and C. Vaillancourt, "Simulation and computer-aided kinematics design of three-degree-of-freedom spherical parallel manipulators," *J. Rob. Syst.* **12**(12), 857–869 (1995).
5. R. I. Alizade, N. R. Tagiyiev and J. Duffy, "A forward and reverse displacement analysis of an in-parallel spherical manipulator," *Mech. Mach. Theory* **29**(1), 125–137 (1994).
6. J. M. Wiitala and M. M. Stanisic, "Design of an overconstrained and dexterous spherical wrist,", *ASME J. Mech. Des.* **122**(3), 347–353 (2000).
7. G. Alici and B. Shirinzadeh, "Topology optimisation and singularity analysis of a 3-SPS parallel manipulator with a passive constraining spherical joint," *Mech. Mach. Theory* **39**, 215–235 (2004).
8. C. Innocenti and V. Parenti-Castelli, "Echelon form solution of direct kinematics for the general fully-parallel spherical wrist," *Mech. Mach. Theory* **28**(4), 553–561 (1993).
9. K. Wohlhart, "Displacement analysis of the general spherical Stewart platform," *Mech. Mach. Theory* **29**(4), 581–589 (1994).
10. M. Karouia and J. M. Herve, "A three-dof tripod for generating spherical rotation," **In**: *Advances in Robot Kinematics* (J. Lenarcic and M. M. Stanisic, eds.), (Kluwer Academic Publishers, Netherlands, 2000) pp. 395–402.
11. R. Di Gregorio, "A new parallel wrist employing just revolute pairs: The 3-RUU wrist," *Robotica* **19**(3), 305–309 (2000).
12. R. Di Gregorio, "Kinematics of a new spherical parallel manipulator with three equal legs: The 3-URC wrist," *J. Rob. Syst.* **18**(5), 213–219 (2001).
13. R. Di Gregorio, "The 3-RRS wrist: A new, simpleand non-overconstrained spherical parallel manipulator," *ASME J. Mech. Des.* **126**, 850–855 (2004).
14. R. Vertechy and V. Parenti-Castelli, "Real-time direct position analysis of parallel spherical wrists by using extra sensors," *ASME J. Mech. Des.* **128**, 288–294 (2006).
15. M. Karouia and J. M. Herve, "Asymmetrical 3-dof spherical parallel mechanisms," *Eur. J. Mech.* **24**, 47–57 (2005).
16. J. J. Cervantes-Sanchez, J. C. Hernandez-Rodriguez and E. J. Gonzalez-Galvan, "On the 5R spherical, symmetric manipulator: workspace and singularity characterization," *Mech. Mach. Theory* **39**, 409–429 (2004).
17. H. R. Mohammadi Daniali, P. J. Zsombor-Murray and J. Angeles, "The kinematics of 3-dof planar and spherical double-triangular parallel manipulators," **In**: *Computational Kinematics* (J. Angeles, G. Hommel and P. Kovacs, eds.) (Kluwer Academic Publishers, Dordecht, 1993) pp. 153–164.
18. C. Gosselin, Kinematic Analysis Optimization and Programming of Parallel Robotic Manipulators, *Ph. D. Thesis* (McGill University, Montréal, Canada, 1988).

Appendix

$$N_8 = F_{10}^2F_1^2 + F_5^2F_6^2 + 6F_{10}F_4F_9F_1 + F_{10}F_4^2F_6 + 5F_{10}F_1F_5F_6 + F_5F_9^2F_1 + 6F_5F_9F_4F_6 \quad (A.1)$$

$$N_7 = 6F_{10}F_4F_9F_2 + F_{10}F_4^2F_7 + 6F_8F_4F_9F_1 + 2F_{10}^2F_1F_2 + 2F_{10}F_1^2F_8 + 5F_{10}F_1F_5F_7 + 5F_{10}F_1F_3F_6 + 5F_{10}F_2F_5F_6 + 5F_8F_1F_5F_6 + 2F_5^2F_6F_7 + 2F_5F_6^2F_3 + F_8F_4^2F_6 + F_5F_9^2F_2 + 6F_5F_9F_4F_7 + F_3F_9^2F_1 + 6F_3F_9F_4F_6 \quad (A.2)$$

$$N_6 = 3F_{10}^2F_1^2 + F_{10}^2F_2^2 + F_8^2F_1^2 + 3F_5^2F_6^2 + F_5^2F_7^2 + F_3^2F_6^2 + 6F_8F_4F_9F_2 + F_{10}F_1F_5F_6 + 4F_{10}F_1F_8F_2 + 5F_{10}F_1F_3F_7 + 5F_{10}F_2F_5F_7 + 5F_{10}F_2F_3F_6 + 5F_8F_1F_5F_7 + 5F_8F_1F_3F_6 + 5F_8F_2F_5F_6 + 4F_5F_6F_3F_7 + 6F_3F_9F_4^*F7 + F_8F_4^2F_7 + F_3F_9^2F_2 \quad (A.3)$$

$$N_5 = 2F_5F_7^2F_3 + 2F_3^2F_6F_7 + 6F_{10}F_4F_9F_2 + F_{10}F_4^2F_7 + F_{10}^2F_1F_2 + F_{10}F_1^2F_8 + 6F_{10}F_1F_5F_7 + 6F_{10}F_1F_3F_6 + 6F_{10}F_2F_5F_6 + 2F_{10}F_2^2F_8 + 5F_{10}F_2F_3F_7 + 2F_8^2F_1F_2 + 6F_8F_1F_5F_6 + 5F_8F_1F_3F_7 + 5F_8F_2F_5F_7 + 5F_8F_2F_3F_6 + F_5^2F_6F_7 + F_5F_6^2F_3 + 6F_3F_9F_4F_6 + 6F_8F_4F_9F_1 + F_8F_4^2F_6 + F_5F_9^2F_2 + 6F_5F_9F_4F_7 + F_3F_9^2F_1 \quad (A.4)$$

$$N_4 = 5F_{10}F_4^2F_6 + 5F_5F_9^2F_1 + 6F_{10}^2F_1^2 + 6F_5^2F_6^2 + 5F_5^2F_7^2 + 5F_8^2F_1^2 + 5F_3^2F_6^2 + F_3^2F_7^2 + F_8^2F_2^2 + 2F_5F_9F_4F_6 + 5F_8F_2F_3F_7 + 2F_{10}F_4F_9F_1 + 2F_{10}F_1F_5F_6 + 5F_{10}^2F_2^2 + 5F_8F_4F_9F_2 + 4F_{10}F_1F_3F_7 + 6F_{10}F_1F_8F_2 + 4F_8F_1F_3F_6 + 4F_8F_2F_5F_6 + 4F_{10}F_2F_5F_7 + 4F_{10}F_2F_3F_6 + 4F_8F_1F_5F_7 + 6F_5F_6F_3F_7 + 5F_3F_9F_4F_7 + 2F_8F_4^2F_7 + 2F_3F_9^2F_2 \quad (A.5)$$

$$N_3 = F_{10}F_4F_9F_2 + 6F_{10}F_4^2F_7 + 6F_{10}^2F_1F_2 + 6F_{10}F_1^2F_8 + F_{10}F_1F_5F_7 + F_{10}F_1F_3F_6 + 5F_{10}F_2^2F_8 + F_{10}F_2F_5F_6 + 2F_{10}F_2F_3F_7 + F_8F_1F_5F_6 + 5F_8^2F_1F_2 + 2F_8F_2F_5F_7 + 2F_8F_2F_3F_6 + 2F_8F_1F_3F_7 + 6F_5^2F_6F_7 + 6F_5F_6^2F_3 + 5F_5F_7^2F_3$$

https://doi.org/10.1017/S0263574708005031 Published online by Cambridge University Press

$$+ F_3F_9F_4F_6 + F_8F_4F_9F_1 + 6F_8F_4^2F_6 + 6F_5F_9^2F_2 + F_5F_9F_4F_7 + 6F_3F_9^2F_1 + 5F_3^2F_6F_7 \quad \text{(A.6)}$$

$$N_2 = 3F_{10}^2F_1^2 + F_{10}^2F_2^2 + F_8^2F_1^2 + 3F_5^2F_6^2 + F_5^2F_7^2 + F_3^2F_6^2 + 6F_8F_4F_9F_2 + F_{10}F_1F_5F_6 + 4F_{10}F_1F_8F_2 + 5F_{10}F_1F_3F_7 + 5F_{10}F_2F_5F_7 + 5F_{10}F_2F_3F_6 + 5F_8F_1F_5F_7 + 5F_8F_1F_3F_6 + 5F_8F_2F_5F_6 + 4F_5F_6F_3F_7 + 6F_3F_9F_4F_7 + F_8F_4^2F_7 + F_3F_9^2F_2 \quad \text{(A.7)}$$

$$N_1 = F_{10}F_4F_9F_2 + 6F_{10}F_4^2F_7 + 5F_{10}^2F_1F_2 + 2F_{10}F_2F_5F_6 + 5F_{10}^{*}F_1^2F_8 + 2F_{10}F_1F_5F_7 + 2F_{10}F_1F_3F_6 + 2F_8F_1F_5F_6 + 5F_5^2F_6F_7 + 5F_5F_6^2F_3 + 6F_3F_9^2F_1 + F_3F_9F_4F_6 + F_8F_4F_9F_1 + 6F_8F_4^2F_6 + 6F_5F_9^2F_2 + F_5F_9F_4F_7 \quad \text{(A.8)}$$

$$N_0 = F_{10}^2F_1^2 + F_5^2F_6^2 + F_{10}F_4^2F_6 + F_5F_9^2F_1 - F_{10}F_4F_9F_1 - 2F_{10}F_1F_5F_6 - F_5F_9F_4F_6 \quad \text{(A.9)}$$

https://doi.org/10.1017/S0263574708005031 Published online by Cambridge University Press